Modeling of Cross-flow Ultrafiltration:

The effects of dispersion transport properties and impermeable membrane segments on concentration-polarization layer

G. W. Park[1], **M. Brito**[1], **E. Zholkovskiy**[2], **and G. Nägele**[1] (e-mail: g.park@fz-juelich.de)

[1] *Institute of Complex Systems, ICS-3, Forschungszentrum Jülich*

[2] *Institute of Bio-Colloid Chemistry, Ukrainian Academy of Sciences, Kiev, Ukraine*

Abstract

Cross-flow filtration is a pressure-driven separation and enrichment process for colloidal dispersions where the feed dispersion is continuously pumped through a membrane pipe. The transmembrane pressure (TMP) causes the solvent to flow out of the membrane, while the colloidal particles are retained inside the pipe. Consequently, a particles-enriched diffusive layer is formed near the membrane wall which reduces the filtration efficiency. This so-called concentration-polarization (CP) layer is determined by the balance of flow advection of particles towards, and gradient diffusion away from the membrane. In the ultrafiltration regime where Brownian motion dominates flow convection, the collective diffusion coefficient and the dispersion viscosity are key transport properties determining the CP layer, in conjunction with the TMP and transmembrane osmotic pressure. In this study, we present a new boundary layer method for the detailed flow and concentration profiles which are compared with simulation results using the finite-element method (FEM) [1]. Results for the filtration and flow efficiency are discussed for different dispersions including impermeable hard spheres (as a reference system), solvent-permeable particles such as non-ionic microgels, and ionic microgels with concentration-dependent size. Furthermore, we generalize the FEM analysis to a segmented membrane with impermeable rings which we observe weakening of the CP layer [2].

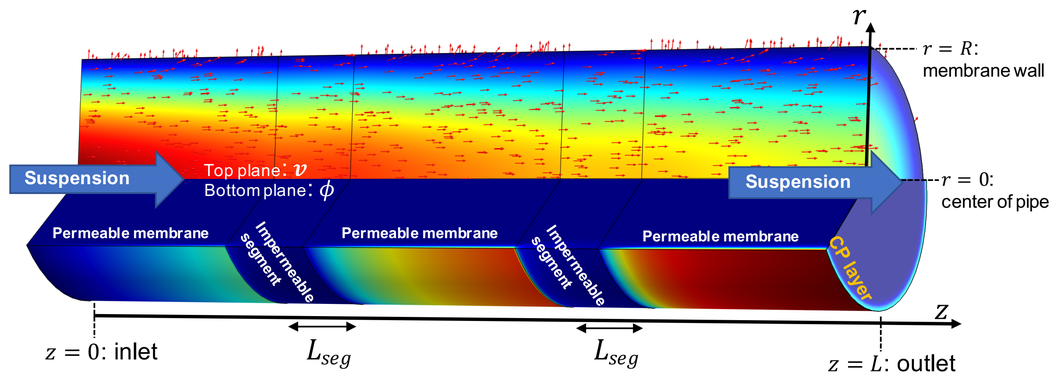

1 Modeling of cross-flow ultrafiltration

1.1 Governing equations

We use the effective Stokes equation for suspension flow

$$\nabla P = \eta(\phi)\nabla^2\mathbf{v} + \nabla\eta(\phi)\cdot\left(\nabla\mathbf{v} + (\nabla\mathbf{v})^T\right)$$

where $\mathbf{v}$ is dispersion-averaged velocity, P is the pressure, and η is suspension viscosity depending on particle volume fraction ϕ.

In ultrafiltration, diffusion of particles is dominated by Brownian motion, which leads to the advection-diffusion equation

$$\frac{\partial\phi}{\partial t} + \mathbf{v}\cdot\nabla\phi = \nabla\cdot(D(\phi)\nabla\phi)$$

where D is the (long-time) collective diffusion coefficient. In this study, the transport properties η and D are given by models of impermeable and solvent-permeable hard spheres [3], and ionic microgels [4, 5].

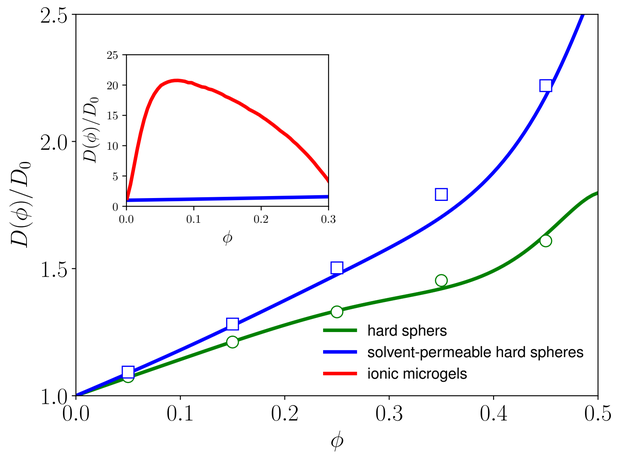

Figure 1: Collective diffusion coefficient of hard spheres (green), solvent-permeable hard spheres (blue), and ionic microgels (red), normalized by diffusion coefficient D_0. Lines are model predictions, and symbols are simulation results for impermeable and solvent-permeable hard spheres[6].

1.2 Permeate flux

The solvent permeable flux is described by the integrated Darcy law

$$v_w(z) = L_p\left(P(z) - P_{perm} - \Pi(\phi_w; z)\right),$$

where $L_p = 6.7\times10^{-10} m/(Pa\,sec)$ is the solvent permeability of the membrane, $P_{perm} = 1\,atm$ is applied constant pressure, and $\Pi(\phi)$ is the osmotic pressure described by the Carnahan-Starling equation.

1.3 Operating conditions

Operating conditions are characterized by the longitudinal pressure difference $\Delta_L P = P_{in} - P_{out}$ and transmembrane pressure (TMP) $\Delta_T P = (1/L)\int_0^L (P(z) - P_{perm})dz$. The reference conditions are $\Delta_T P$=5 kPa and $\Delta_L P = 130$ Pa.

1.4 Boundary conditions

- (center) Axisymmetry: $v(r=0,z)=0$
- (wall) Darcy's law: $v(r=R,z) = v_w(z)$
- (wall) No slip along z: $u(r=R,z)=0$
- (wall) No particle flux: $-\hat{\mathbf{r}}\cdot\mathbf{j}_\phi(r=R,z)=0$
- (inlet) Particle: $\phi(r,z=0)=\phi_b$
- (inlet and outlet) Pressure: $P(r,z=0)=P_{in}$, $P(r,z=L)=P_{out}$

1.5 Finite element method (FEM)

- We use Comsol Multiphysics with *laminar flow* and *transport of dilute species* packages, using a time-dependent solver for the advection-diffusion equation
- P1/P1 elements for $\mathbf{v}$ and P, and P2 element for ϕ
- Meshes are stretched along z axis

2 Homogeneous membrane pipe

2.1 Pure solvent flow

An analytic solution is obtained using a zeroth-order regular perturbation expansion with $\epsilon = R/L = 10^{-3}$ and $\epsilon Re \ll 1$ [1].

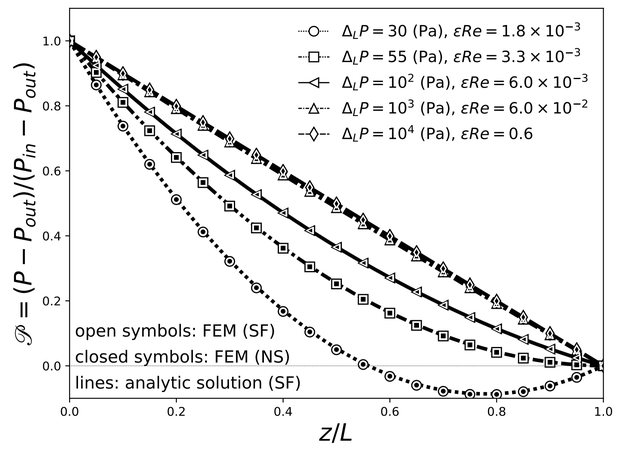

Figure 2: Analytic pressure distribution (lines), the corresponding FEM results (open symbols), and the Navier-Stokes solution for steady-state (closed symbols) pure solvent flow with $\Delta_L P = 30$, 55, 100, 1000, and 10000 (Pa) as indicated.

2.2 Reference suspension

We obtained a semi-analytic flow and concentration profiles by matching the inner solution using singular perturbation expansion with $\epsilon_\delta = \delta/R$, to the outer solution for modified pure solvent flow. We compare our new boundary layer analysis (mBLA) with FEM and a similarity solution proposed in [7] (sBLA), for the reference suspensions.

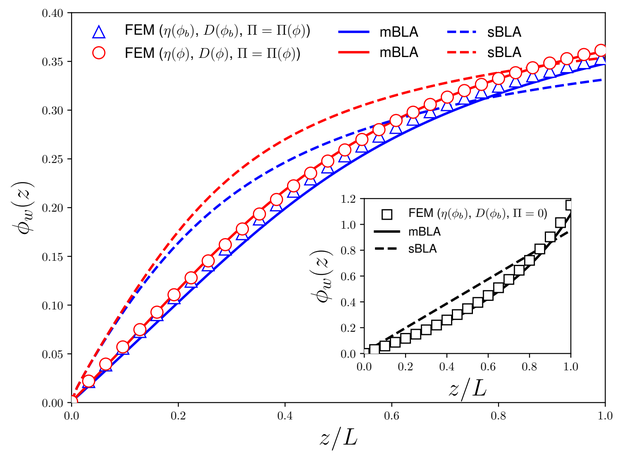

Figure 3: Particle concentration at membrane (ϕ_w): comparison between FEM (symbols), matched asymptotic solution of new BLA (mBLA; solid lines), and similarity solution of previous BLA in [7] (sBLA; dashed lines). The suspension properties are characterized by the constant (blue) and concentration-dependent η and D (red). Inset shows ϕ_w for constant η and D with neglecting the osmotic pressure values.

2.3 Effect of suspension properties (mBLA study)

The mBLA method is applicable also for the concentration-dependent η, D, and Π. Different dispersions are analyzed by the flow efficiency, Q_{perm}/Q^0_{perm}, where $Q_{perm} = 2\pi R\int_0^L v_w(z)dz$ and $Q^0_{perm} = 2\pi RLL_P\langle\Delta_T P\rangle$.

Figure 4: Flow efficiency as function of transmembrane pressure, $\Delta_T P$, for three types of dispersions: impermeable hard spheres (green), solvent-permeable hard spheres (blue), and ionic microgels (red). Inset shows the particle wall concentration ϕ_w along z at $\Delta_T P = 5\,(kPa)$.

3 Segmented membrane (FEM study)

We add impermeable segments to the membrane, for which the absence of permeate flux reduces the intensity (ϕ_w) of the CP layer. As shown, the overall effect of the segmentation is minor because of quick recovery of the CP layer following impermeable rings. This memory effect is quantified by FEM calculations.

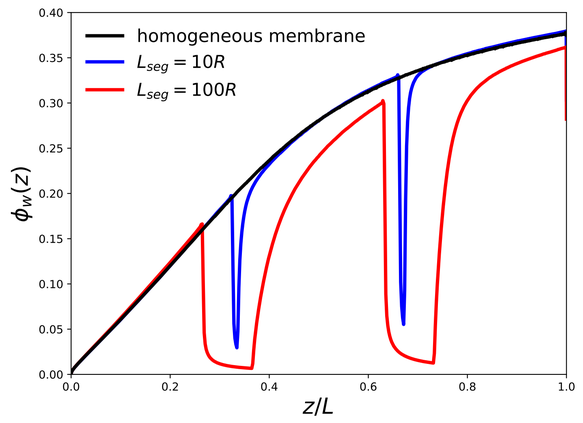

Figure 5: Membrane wall concentration of particles a homogeneous membrane (black), and a membrane with impermeable rings of length $L_{seg} = 10R$ (blue), and $L_{seg} = 100R$ (red), for a hard-sphere suspension.

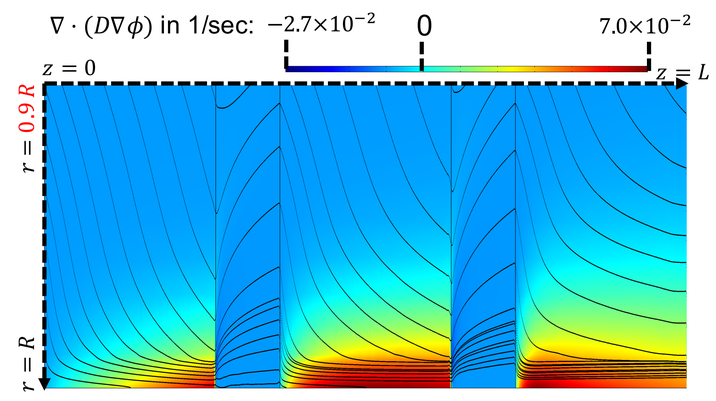

Figure 6: Diffusive flux contribution $\nabla\cdot(D\nabla\phi)$ (colors), and streamlines of the particle flux $\mathbf{j}_\phi = \phi\mathbf{v} - D\nabla\phi$ (lines) near a membrane wall for $0.9R \le r \le R$.

Concluding Remarks

1. Our new mBLA solutions for the concentration profile are in quantitative good agreement with FEM results which supports the validity of the both methods; the result by the sBLA [7] systematically overestimate ϕ_w.
2. The CP layer for different dispersions are analyzed based on the flow efficiency (Fig. 4). Strong deviations between charged and neutral particles are observed because of differences in the collective diffusion coefficient (Fig. 1).
3. For a segmented membrane, a weakening of the CP layer is observed since the particles in the segments are diffusing away from the membrane wall. The particles, however, remain near to the wall (Fig. 6) causing a quick recovery of the CP layer. Overall, flow efficiency is not enhanced by segmentation.

Acknowledgments

The authors gratefully acknowledge financial support by the Deutsche Forschungsgemeinschaft (SFB-985, Project B6).

References

[1] G. W. Park and G. Nägele, "Analytical and numerical approaches of concentration-polarization layers for cross-flow ultrafiltration in a cylindrical membrane pipe", manuscript in preparation.

[2] G. W. Park, M. Brito, E. K. Zholkovskiy, and G. Nägele, work in progress.

[3] J. Riest, T. Eckert, W. Richtering, and G. Nägele, "Dynamics of suspensions of hydrodynamically structured particles: analytic theory and applications to experiments", Soft Matter **11**, 2821–2843 (2015).

[4] G. Nägele, "Dynamics of soft and permeable particles suspensions", 6th June, **Session C, ISMD 2019**.

[5] M. Brito, A. Denton, and G. Nägele, "Deswelling effects on structural and dynamic properties of ionic microgel suspensions", **Poster Session, ISMD 2019**.

[6] G. C. Abade, B. Cichocki, M. L. Ekiel-Jeżewska, G. Naegele, and E. Wajnryb, "Short-time dynamics of permeable particles in concentrated suspensions", Journal of Chemical Physics **132**, 014503–18 (2010).

[7] R. Roa, E. K. Zholkovskiy, and G. Nägele, "Ultrafiltration modeling of non-ionic microgels", Soft Matter **11**, 4106–4122 (2015).